COMPUTATIONAL BIOLOGY

The Mammalian MAPK/ERK Pathway Exhibits Properties of a Negative Feedback Amplifier

Oliver E. Sturm,[1*†] Richard Orton,[1*‡] Joan Grindlay,[2*] Marc Birtwistle,[3] Vladislav Vyshemirsky,[1§] David Gilbert,[1‖] Muffy Calder,[1] Andrew Pitt,[4] Boris Kholodenko,[3] Walter Kolch[3,5¶]

(Published 21 December 2010; Volume 3 Issue 153 ra90)

Three-tiered kinase modules, such as the Raf–MEK (mitogen-activated or extracellular signal–regulated protein kinase kinase)–ERK (extracellular signal–regulated kinase) mitogen-activated protein kinase pathway, are widespread in biology, suggesting that this structure conveys evolutionarily advantageous properties. We show that the three-tiered kinase amplifier module combined with negative feedback recapitulates the design principles of a negative feedback amplifier (NFA), which is used in electronic circuits to confer robustness, output stabilization, and linearization of nonlinear signal amplification. We used mathematical modeling and experimental validation to demonstrate that the ERK pathway has properties of an NFA that (i) converts intrinsic switch-like activation kinetics into graded linear responses, (ii) conveys robustness to changes in rates of reactions within the NFA module, and (iii) stabilizes outputs in response to drug-induced perturbations of the amplifier. These properties determine biological behavior, including activation kinetics and the response to drugs.

INTRODUCTION

Three-tiered kinase modules are a common motif in signal transduction pathways that enable precise cellular responses to extracellular cues. The prototypic mitogen-activated protein kinase (MAPK) cascades consist of a guanosine triphosphatase (GTPase)–regulated initial kinase [MAPK kinase kinase (MAPKKK)], which phosphorylates and activates an intermediate kinase (MAPKK) with narrow substrate specificity that phosphorylates and activates the third kinase (MAPK), which is the main pathway effector and usually has multiple substrates (*1*). The biological reason for this design is unclear. Theoretical considerations suggest that it enables high signaling rates and amplification while providing stable off states (*2*). Negative feedback loops (NFLs) are predicted to add rich dynamic properties to signaling pathways, such as oscillations and switch-like responses (*3*). In metabolic pathways, NFLs stabilize end-product concentrations with respect to changes in consumption rates or substrate input supplies (*4*). Combining experimental and mathematical analysis, we show that the integration of a kinase cascade amplifier with NFLs generates emergent system-level properties that resemble the negative feedback amplifier (NFA) known from engineering, and that these NFA-like properties affect drug sensitivity and adaptation to perturbations of cells. We analyzed the extracellular signal–regulated kinase (ERK) MAPK pathway, which regulates fundamental cellular processes including proliferation, survival, transformation, differentiation, and motility (*5*, *6*). ERK signaling is initiated by cell surface receptors that activate Ras by recruiting guanine nucleotide exchange factors, such as SOS, which load Ras with guanosine triphosphate (GTP) (*5*, *7*, *8*). RasGTP binds MAPKKKs of the Raf family with high affinity, translocating them from the cytosol to the cell membrane where they become activated. Active Raf phosphorylates and activates mitogen-activated or extracellular signal–regulated protein kinase kinase (MEK), which in turn phosphorylates and activates ERK.

[1]Department of Computing Science, University of Glasgow, Glasgow G12 8QQ, UK. [2]Signalling and Proteomics Laboratory, Beatson Institute for Cancer Research, Garscube Estate, Switchback Road, Glasgow G61 1BD, UK. [3]Systems Biology Ireland, University College Dublin, Belfield, Dublin 4, Ireland. [4]Sir Henry Wellcome Functional Genomics Facility, University of Glasgow, Glasgow G12 8QQ, UK. [5]Conway Institute, University College Dublin, Belfield, Dublin 4, Ireland.
*These authors contributed equally to this work.
†Present address: Department of Immunology, St. Jude Children's Research Hospital, Memphis, TN 38104, USA.
‡Present address: Comparative Epidemiology Group, Faculty of Veterinary Medicine, University of Glasgow, Glasgow G61 1QH, UK.
§Present address: Department of Mathematics and Statistics, University of Strathclyde, Glasgow G1 1XH, UK.
‖Present address: School of Information Systems, Computing and Mathematics, Brunel University, Uxbridge, Middlesex UB8 3PH, UK.
¶To whom correspondence should be addressed. E-mail: walter.kolch@ucd.ie

RESULTS

The NFA design and experimental approaches to examine NFA-like properties of the Raf-MEK-ERK pathway

In engineering, the NFA design (Fig. 1A) is widely used for controlling dynamic processes to reduce the effects of input noise, buffer perturbations in the amplifier, and smoothen output responses (*9*, *10*). In a Raf-MEK-ERK biological circuit, the input signal coming from receptors proceeds through activated RasGTP to the amplifier, represented by the Raf-MEK-ERK module (Fig. 1B). The ratio of protein abundances of Raf-1, MEK, and ERK is about 1:3:6 in COS cells and 1:0.7:9 in NIH 3T3 fibroblasts (fig. S1), thus permitting signal amplification. A direct NFL from ERK to SOS, involving its phosphorylation and inhibition (*11*), inhibits Ras activation, and another NFL involves Raf-1 phosphorylation and inhibition (*12*) by activated ERK. A key property of an NFA is to convey robustness against perturbations to the amplifier (Fig. 1C), while still linearly transmitting input signals (Fig. 1D). To explore the NFA properties of the ERK pathway, we modeled it as either a simple amplifier ("Feedback Broken") or an NFA ("Feedback Intact"), using ordinary differential equations (Supplementary Materials, sections 1.1 and 1.2, and fig. S2). The Feedback Intact model starts with Ras as the input reflecting Raf stimulation by different growth factors and ends with ERK activity, as measured by ERK phosphorylation, as output. To test the predictions of this model experimentally, we used two strategies to eliminate the NFLs (Fig. 1E and fig. S3). Introduction of Raf6A, a Raf-1 mutant

where all six ERK phosphorylation sites are replaced by alanines (*12*), eliminated the feedback from ERK to Raf6A, but not the feedback to SOS or to endogenous Raf-1. Both feedback loops were eliminated if the pathway was activated by BXB-ER, which consists of the kinase domain of Raf-1 (BXB) fused to the hormone-binding domain of the estrogen receptor (ER) (*13*). The kinase activity of BXB-ER is directly activated by 4-hydroxy-tamoxifen (4HT), bypassing growth factor receptors and Ras proteins (*13*). BXB-ER lacks five of the six ERK phosphorylation sites, rendering it resistant to negative ERK feedback regulation. To ensure that the results were directly comparable, we calibrated (i) the mathematical model to provide equal input strengths through Raf-1 activated by RasGTP and BXB-ER activated by 4HT (Supplementary Materials, section 1.3), leaving the other parameters the same; and (ii) the biological system by titrating 4HT to adjust the kinase activity of BXB-ER to that of endogenous Raf-1 activated by epidermal growth factor (EGF)–stimulated RasGTP accumulation (Fig. 1F), and by expressing Raf6A at similar abundance as a wild-type Raf-1 control (fig. S4). Exposure of EGF- or 4HT-stimulated cells to the MEK inhibitor U0126 (*14*, *15*) had no effect on BXB-ER activity, but prolonged the activity of Raf-1. Cells expressing Raf6A had slightly increased basal kinase activity, which was stimulated by EGF but, in contrast to Raf-1, was sustained even in the absence of U0126 (Fig. 1F). These results showed that the negative feedback limits the duration of Raf-1 activation and that our experimental tools are suitable to interrogate the NFA design.

Conversion of switch-like ERK activation into a graded response by the NFA-like design

In the ERK pathway, amplifier distortions arise naturally because MEK phosphorylates each of the two sites required for full ERK activity separately rather than processively during one binding event (*16*, *17*). As a result, the single-phosphorylated, low-activity form of ERK is generated during the initial activation phase. When enough single-phosphorylated ERK has accumulated, every new phosphorylation event produces double-phosphorylated, fully activated ERK, which is apparent as a steep nonlinear increase in ERK activation kinetics (*18*). This hypersensitive mode of activation changes the internal gain of the amplifier in a nonlinear fashion, resulting in a switch-like response, which is predicted by our mathematical model (Fig. 2A), and was observed experimentally in *Xenopus* oocytes

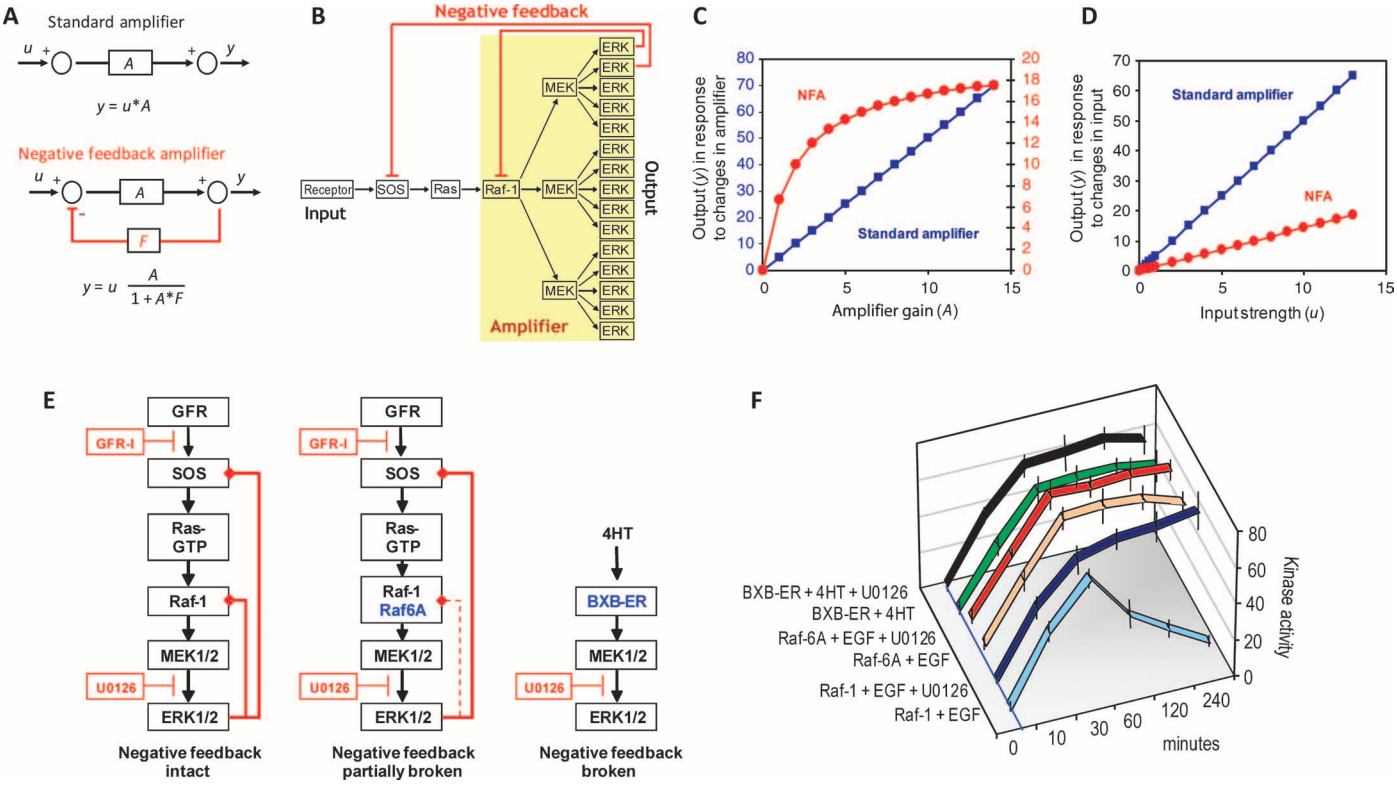

Fig. 1. The ERK pathway resembles a negative feedback amplifier (NFA). (**A**) Blueprint of a standard amplifier and an NFA; *u* = input; *y* = output; *A* = amplification; *F* = feedback. (**B**) The ERK pathway resembles an NFA with an amplifier consisting of the three-tiered kinase module Raf-MEK-ERK and feedbacks emanating from ERK to SOS and Raf-1 activation. (**C**) Simulation of signal input-output relationships (*u*/*y*) in regard to changes in the amplifier (amplification strength, *A*) for a standard amplifier (blue line and blue *y*-axis labels) and an NFA (red line and red *y*-axis labels). (**D**) Simulation of signal input-output relationships in regard to changes in input (*u*) signals in a standard amplifier (blue line) and an NFA (red line). (**E**) Strategies to break the NFA. GFR, growth factor receptor; GFR-I, GFR inhibitors; U0126, MEK inhibitor; solid red lines ending in diamonds represent negative feedback interactions; dashed red lines ending in diamonds indicate partial loss of negative feedback; blue molecules indicate introduced mutant or fusion proteins. (**F**) Kinase activities of Raf-1 and Raf-1 mutants. Flag-tagged Raf-1 and Raf6A or HA-tagged BXB-ER was expressed in COS1 cells. Serum-starved cells were treated with 10 μM U0126 before stimulation with EGF (50 ng/ml) or 0.1 μM 4HT. At the indicated time points, tagged Raf proteins were immunoprecipitated and assayed for kinase activity. Error bars represent SEM (*n* = 4).

(*19*). According to our mathematical NFA model simulations (Fig. 2A), the negative feedback should convert the switch-like, hypersensitive response into a more graded response by reducing the sensitivity of the reactions in the amplifier module to perturbations (Fig. 2A). To test this prediction theoretically, we performed sensitivity analysis of the mathematical model (Fig. 2B and Supplementary Materials, section 1.5). Sensitivity coefficients provide a quantitative measurement of how changes in individual reactions affect the output, here measured as the abundance of doubly phosphorylated ERK (ppERK). Elimination of the negative feedback increased the sensitivity coefficients of most reactions in the amplifier module, especially the reactions that activate and deactivate MEK. This increase in the sensitivity coefficients in the amplifier module is explained by the mathematical model because the strength of the negative feedback is directly coupled to the gain of the amplifier, which corrects variations in the parameters in the amplifier module. Thus, the biological NFA allowed signal amplification but made the system resilient to amplifier perturbations.

The theoretical analysis of the NFA model predicted that ERK activation should be switch-like in the absence of negative feedback, but graded when it is present. To test this prediction experimentally, we analyzed ERK activation by flow cytometry, which measures ERK activity in individual cells of a population (Fig. 2C). In the Feedback Intact system, ERK activation increased in a graded manner proportional to the stimulation. However, in the Feedback Broken system, the response be-

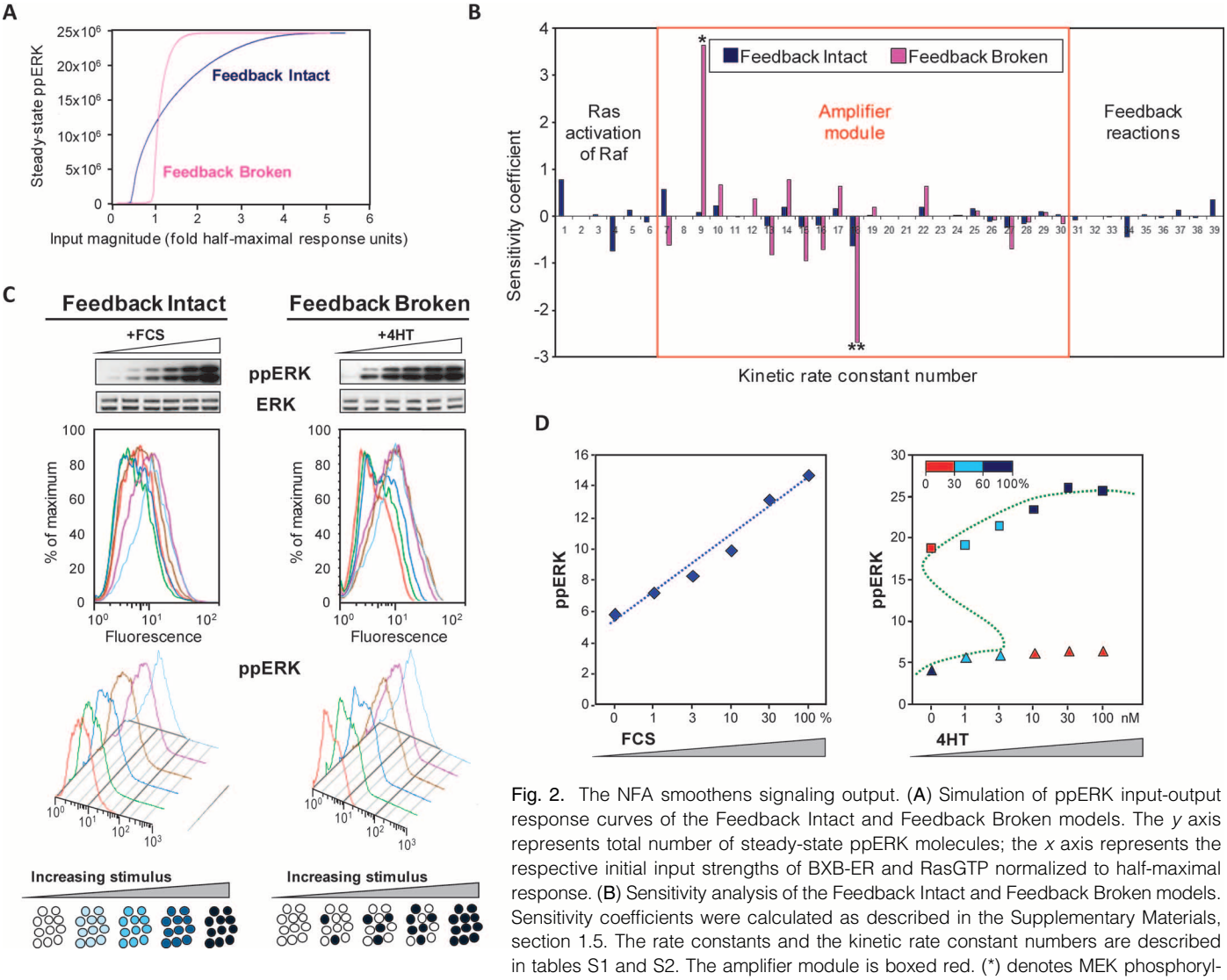

Fig. 2. The NFA smoothens signaling output. (**A**) Simulation of ppERK input-output response curves of the Feedback Intact and Feedback Broken models. The *y* axis represents total number of steady-state ppERK molecules; the *x* axis represents the respective initial input strengths of BXB-ER and RasGTP normalized to half-maximal response. (**B**) Sensitivity analysis of the Feedback Intact and Feedback Broken models. Sensitivity coefficients were calculated as described in the Supplementary Materials, section 1.5. The rate constants and the kinetic rate constant numbers are described in tables S1 and S2. The amplifier module is boxed red. (*) denotes MEK phosphorylation by Raf-1; (**) denotes MEK dephosphorylation. (**C**) NFA effects on ERK activation kinetics. NIH 3T3 cells stably expressing BXB-ER (*31*) were stimulated with increasing amounts of 4HT (0, 1, 3, 10, 30, and 100 nM) or fetal calf serum (FCS; 0, 1, 3, 10, 30, and 100%) for 20 min. ERK phosphorylation (ppERK) was determined by Western blotting and flow cytometry analysis. The data are representative of three independent experiments, in each of which 10^5 cells were analyzed. The schematic at the bottom illustrates the interpretation of the data. (**D**) Means of the ppERK fluorescence intensity distributions from (C) are plotted as a function of FCS or 4HT concentration. Triangles and squares represent the first and second peaks in the bimodal 4HT distribution, respectively. The color bar represents the percentage of cells in each category.

came switch-like, in which individual cells either responded or not, and the number of responding cells increased in proportion to the stimulation. Thus, the presence or absence of the NFLs can determine whether the response of the kinase module is graded or switch-like (Fig. 2D). This may explain divergent results about the activation kinetics of the ERK cascade in different biological systems. Although it has switch-like properties in *Xenopus* oocytes (*19*), subsequent studies in mammalian cells found that it responded in a graded fashion (*20*, *21*). In *Xenopus* oocytes, the main mitotic activator of the ERK module is not Raf-1 but c-Mos (*22*). c-Mos lacks the Ras-binding domain and the ERK phosphorylation sites, and hence is not subjected to negative feedback regulation by ERK, resulting in switch-like ERK activation dynamics. However, in mammalian cells in which Raf-1 activates MEK, growth factor stimulation permits the NFA properties to buffer the intrinsic hypersensitivity of the amplifier and generate a graded response.

The NFA-like design and drug sensitivity

Another salient prediction of the NFA model is that ERK activation should be resilient to disturbances of the amplifier (Fig. 1C). To test this prediction, we used the MEK-selective inhibitor U0126 (*14*, *15*). Computational simulations of U0126 dose-response curves predicted high sensitivity of ERK activation to MEK inhibition in the absence of NFLs (Feedback Broken) and resistance to MEK inhibition in the presence of the NFA (Feedback Intact) (Fig. 3A). To test this prediction, we treated cells having the negative feedback either intact or broken with varying amounts of the MEK-selective inhibitor U0126, stimulated them with either EGF (Feedback Intact) or 4HT (Feedback Broken), and then measured ERK activation (*14*, *15*). As predicted by our model, in the Feedback Broken system, ERK activation was thoroughly inhibited by low concentrations of U0126, whereas in the Feedback Intact system, ERK activity persisted even in the presence of high U0126 concentrations (Fig. 3B). With the negative feedback intact, increasing U0126 concentrations weakened the negative feedback and allowed the amplifier gain to rise, thus causing increased resistance to U0126. As inhibitor concentrations were increased further, resistance persisted until U0126 concentrations were high enough to achieve complete inhibition.

We also observed enhanced sensitivity to low U0126 concentrations in the Feedback Intact system. This effect can be explained by three mechanisms, which can operate separately or jointly depending on conditions and inhibitor properties. First, low inhibitor concentrations are inherently associated with linear inhibition kinetics that precede the flattening out of the inhibition curve when rising inhibitor concentrations push the system toward saturation. Linear inhibition ranges are generally larger for tightly bound inhibitors, such as U0126 (*15*). Second, the allosteric mode of inhibition by U0126 fixes MEK in a nonfunctional conformation and prevents MEK from interacting with ERK (*23*). Thus, U0126 not only prevents MEK from binding to ERK but also disrupts MEK-ERK complexes (reactions 27 to 35 in table S1), making inhibition more efficient. Third, if the concentration of ppERK is larger than the abundance of the upstream activator Raf-1 (fig. S1), the negative feedback becomes saturated. In this last scenario, a large reduction of ppERK would be required before Raf-1 inhibition eased and the feedback weakened to allow the increase of input to compensate for the inhibition.

The sensitivities to MEK inhibition that we observed in the computational simulations were obtained with the parameter values from the model by Schoeberl *et al*. (*24*). To test whether variations in the concentrations of Raf-1, MEK, and ERK affected the model, we used the concentrations determined in COS1 cells (fig. S1). The results showed that the effects of MEK inhibition in the Feedback Intact and Feedback Broken models (fig. S5) were similar to those in the simulations in Fig. 3B. In conjunction with the experiments shown in Fig. 2, C and D, where we enhanced the activity of the amplifier module, the inhibition experiments shown in Fig. 3, A and B, demonstrated that the NFA-like design of the ERK pathway conveyed resistance to perturbations of the amplifier caused by increasing concentrations of the MEK inhibitor. These results also showed that the biological circuit is more complex than the classic electronic circuit. One main difference is the temporal element of feedback regulation, which is immediate in the classic electronic NFA, but can be delayed or operating on different parallel time scales in the biological design. Because the effects of U0126 included parallel effects that can occur on different time scales, we tested a situation where U0126 was applied at the peak of ERK activation (fig. S6). In the Feedback Broken system, U0126 caused full ERK inhibition, whereas the Feedback Intact system exhibited dampened inhibition, resulting in a partial recovery to a new steady state of ERK activity above the basal activity. These results suggest that the NFA-like design of biological systems can dynamically buffer amplifier perturbations over time.

The model also predicts that inhibition of components that are not part of the biological NFA should be more effective than inhibition of components within the NFA (Fig. 3A). This prediction was corroborated by comparing the effects of 4557W, an EGF receptor (EGFR) inhibitor, with that of U0126 (Fig. 3B). Inhibition of EGFR produced an almost linear dose-response relationship both in the model and in the experimental system. This suggests that proteins embedded in NFA-like topologies make suboptimal drug targets, because the effects of their inhibition are dampened.

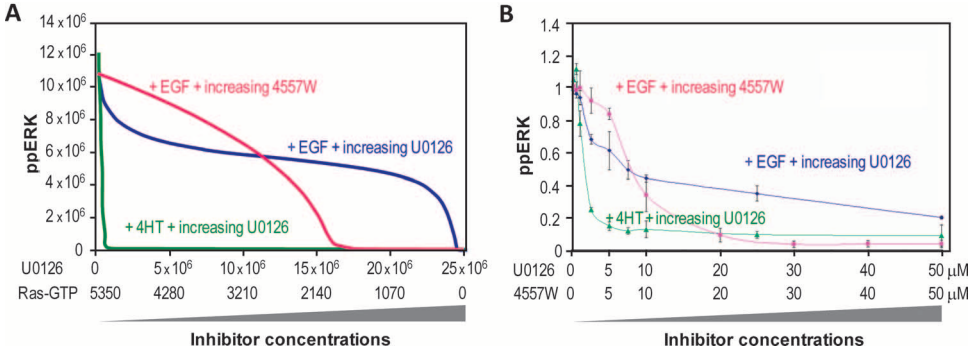

Fig. 3. The NFA-like property determines the responses of the ERK pathway to drugs that inhibit different components of the pathway. (**A**) Predicted sensitivity profiles to MEK (U0126) and EGFR (4775W) inhibitors. The *y* axis represents numbers of ppERK molecules. U0126 was modeled as an allosteric inhibitor, and concentrations are given as number of molecules. The effects of 4775W were modeled as a decrease in the number of RasGTP molecules. (**B**) Measured sensitivity profiles to U0126 and 4775W inhibitors. COS1 cells stably expressing BXB-ER cells were treated with U0126 or 4775W for 1 hour and subsequently stimulated with EGF or 4HT for 20 min. The *x* axis shows inhibitor concentrations, and the *y* axis arbitrary response units based on quantitative LI-COR analysis of Western blot measurements of phosphorylated ERK (ppERK). Data represent the average of three experiments; error bars are SD.

We also tested the effects of the biological NFA with the "Feedback Partially Broken" system based on the Raf6A mutant (*12*) to partially break the negative feedback. Unfortunately, due to cytotoxic effects, we could not obtain cells expressing Raf6A alone in the absence of endogenous Raf-1. Therefore, we used COS1 cells stably expressing similar amounts of Raf-1 or Raf6A (fig. S4). These cells were stimulated with EGF and treated with increasing doses of U0126. In response to EGF stimulation, cells expressing Raf6A were more sensitive to MEK inhibition than were cells expressing Raf-1 (Fig. 4A, upper left). To examine the specificity of the NFA-like effect, we tested different growth factors, in particular platelet-derived growth factor (PDGF) and insulin-like growth factor 1 (IGF-1), factors for which COS1 cells have receptors. PDGF-activated ERK showed an NFA-like response that was similar but smaller than the response to EGF, with cells expressing Raf6A showing decreased resistance to U0126 (Fig. 4A, upper right) but not to a PDGF receptor inhibitor (Fig. 4A, lower left), compared to cells expressing Raf-1. The smaller NFA-like effect seen with the inhibitor of the NFA component MEK can be explained by the lesser ability of PDGF to activate ERK (fig. S7), which weakens the influence of the NFA (Fig. 1A). Curiously, stimulation of ERK by IGF-1 did not exhibit the NFA-like property that partial loss of negative feedback made the MEK inhibitor more effective in reducing ERK activation (Fig. 4A, lower right). We found that IGF-1 selectively activated B-Raf and not Raf-1 (Fig. 4B). Although ERK can phosphorylate B-Raf and induce the disassembly of B-Raf–Raf-1 heterodimers at late time points, acute B-Raf activation is not inhibited by ERK (*25*) (fig. S8). Hence, IGF-1–induced ERK activation is not protected from U0126 inhibition by the NFA-like effect from ERK to Raf-1: This feedback may not exist because IGF-1 does not activate Raf-1, or if B-Raf signaling leading to ERK activation does result in ERK phosphorylation of Raf-1, then this phosphorylation will have no consequences for IGF-1 responses. These results suggest that the NFA model applies to ERK activated downstream of Raf-1, but not B-Raf, which is consistent with the observation that cancer cells harboring mutated B-Raf are highly susceptible to MEK inhibitors (*26*, *27*). The susceptibility of cancers with B-Raf mutations to MEK inhibitors may be due to the lack of negative feedback buffering of MEK inhibition, leading to effective inhibition of ERK activation. Results demonstrating a switching from B-Raf to Raf-1 as the main activator of the ERK pathway in melanoma (*28*) highlight the possibility that this switch could be accompanied by increased resistance to MEK inhibitors due to the acquisition of NFA-like properties. Our results predict that breaking the NFA is essential to ensure sensitivity to MEK inhibitors.

Therefore, we used our model to suggest scenarios for disabling the biological NFA. One possibility is to inhibit targets outside of the biological NFA (Figs. 3, A and B, and 4A). An alternative prediction of the mathematical NFA model was that Raf-1 inhibition should sensitize the pathway to MEK inhibition by weakening the NFA effect (Fig. 5A). This prediction seems counterintuitive because Raf-1–MEK–ERK is a linear activation cascade. However, as predicted by the NFA model, the Raf-1 inhibitor GW5074 increased the sensitivity to MEK inhibition in the Feedback Intact system (Fig. 5B, left). The cooperative effects of Raf and MEK inhibition were absent in the Feedback Broken system (Fig. 5B, right).

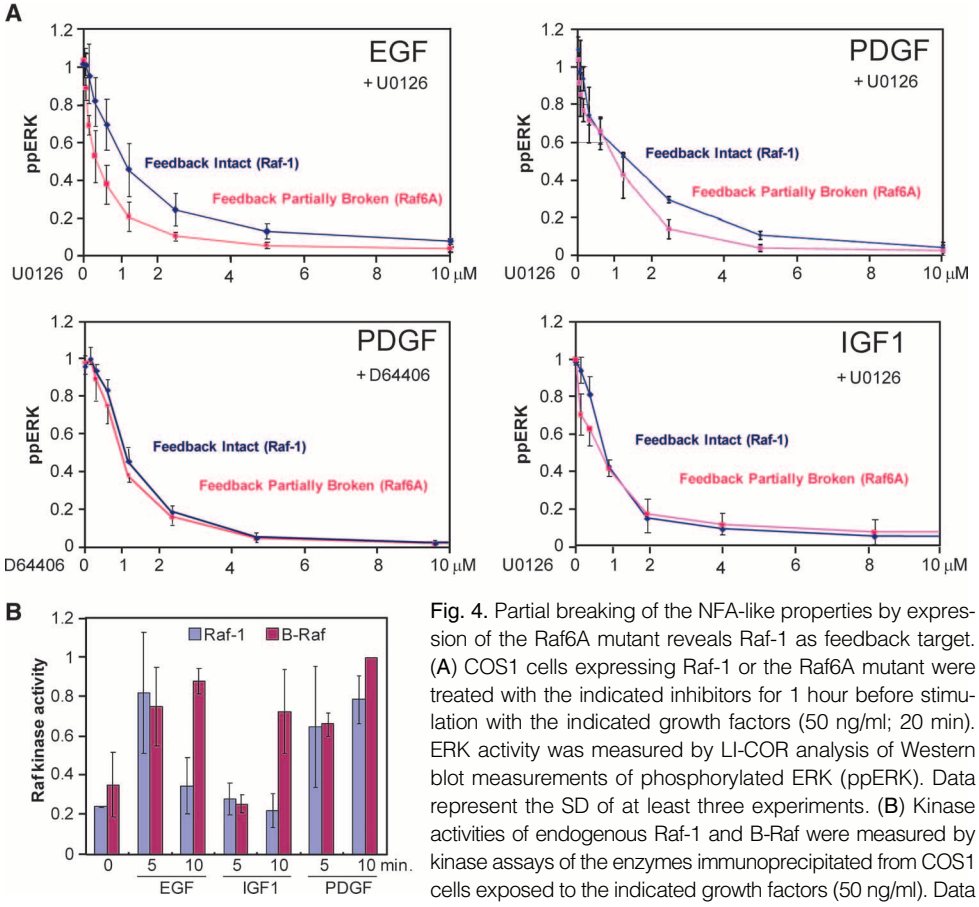

Fig. 4. Partial breaking of the NFA-like properties by expression of the Raf6A mutant reveals Raf-1 as feedback target. (A) COS1 cells expressing Raf-1 or the Raf6A mutant were treated with the indicated inhibitors for 1 hour before stimulation with the indicated growth factors (50 ng/ml; 20 min). ERK activity was measured by LI-COR analysis of Western blot measurements of phosphorylated ERK (ppERK). Data represent the SD of at least three experiments. (B) Kinase activities of endogenous Raf-1 and B-Raf were measured by kinase assays of the enzymes immunoprecipitated from COS1 cells exposed to the indicated growth factors (50 ng/ml). Data represent the SD of at least three experiments.

DISCUSSION

These results suggest that the ERK pathway has intrinsic design features like that of an NFA. Although the biological circuitry differs from the engineering blueprint by its greater complexity and nonlinearity, it conveys salient NFA properties including graded response characteristics, robustness to change, and output stabilization. These have important implications for the regulation of the pathway and the design of inhibitors. For instance, the presence of the negative feedback dictates whether ERK activation follows a graded or a switch-like pattern, as demonstrated by the differences in ERK activation responses when the negative feedback is broken (Fig. 2, B to D). Thus, the biological NFA provides a mechanism to generate analog or digital responses. Another implication is in the choice of targets for pharmacological intervention. Signal transduction pathways are important drug targets (*29*, *30*). However, it has proven difficult to predict which components should be targeted, and the cornucopia of potential drug targets is contrasted by a paucity of objective criteria for how to choose

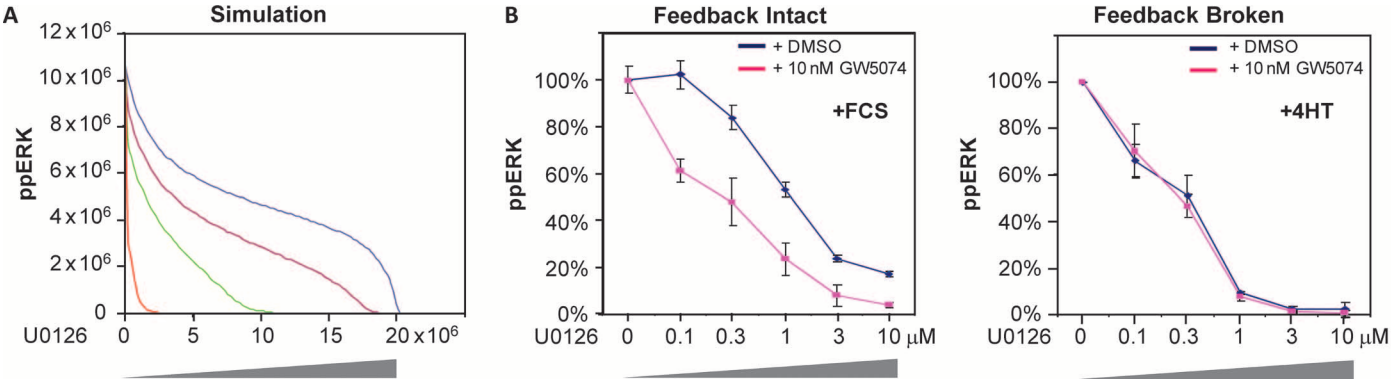

Fig. 5. Cooperation between Raf and MEK inhibitors. (**A**) Model predictions of ppERK abundance at different combinations of Raf (GW5074) and MEK (U0126) inhibitors. The *y* and *x* axes show numbers of ppERK and U0126 molecules, respectively. (**B**) Serum-starved NIH 3T3 BXB-ER cells (*31*) were treated with 10 nM Raf-1 inhibitor (GW5074) and various amounts of the MEK inhibitor U0126 for 60 min and then stimulated with 10% FCS or 100 nM 4HT for 15 min. ppERK was measured by quantitative LI-COR analysis of Western blot measurements of phosphorylated ERK. Error bars represent the SD from the mean of triplicate points.

among them. Our results suggest that inhibition of a pathway by inhibiting targets embedded in an NFA-like topology is more difficult to achieve than the effect of inhibiting targets outside of the feedback loop, which provides a simple drug target selection guideline that is deductible from the network structure. The NFA-like properties also suggest that drugs that inhibit targets within the NFA circuit may be more effective if the NFLs are also blocked or inhibited, thus providing insight into potentially effective combination therapies. On a more speculative note, the results also suggest that biological evolution and engineered systems may converge to similar solutions when designing robustness.

MATERIALS AND METHODS

Reagents and plasmids

Growth factors, drugs, and pharmacological inhibitors were from commercial sources and used according to suppliers' recommendations or as indicated. Antibodies that recognize phosphorylated ERK1 and 2 (ERK1/2) and antibodies that recognize ERK1/2 for immunoblotting were purchased from Cell Signaling. Antibodies that recognize C-Raf-1 and antibodies that recognize hemagglutinin (HA) for immunoprecipitation were purchased from BD Biosciences and Roche, respectively.

Cell culture

Stable BXB-ER NIH 3T3 cells were described (*31*), and COS1 cell lines stably expressing BXB-ER were generated similarly.

Dose-response curves

BXB-ER COS1, NIH 3T3 wild-type-Raf-1, or NIH 3T3 6A-Raf-1 cells were starved in serum-free medium overnight. The cells were preincubated with the indicated amounts of inhibitors U0126, 4557W, or D-64406 for 1 hour and subsequently stimulated with growth factors (50 ng/ml) or 0.1 μM 4HT. The stimulation was stopped by washing the cells with ice-cold phosphate-buffered saline and immediate freezing at −80°C.

Immunoprecipitation, immunoblotting, and immunocomplex kinase assays

Cells were treated with growth factors with or without inhibitors as indicated and lysed in 25 mM Hepes (pH 7.4), 50 mM NaCl, 5 mM EDTA, and 1% Triton X-100 supplemented with protease inhibitor cocktail (Roche) and phosphatase inhibitors (2 mM NaF, 0.2 mM NaP_2O_5, 0.5 mM sodium orthovanadate, and 10 mM β-glycerophosphate). Immunoprecipitations, Western blotting, and kinase assays were performed as described (*25*). Western blots were developed and scanned with LI-COR technology (http://www.licor.com/bio/index.jsp), which is a quantitative technique for staining Western blots based on infrared imaging.

Fluorescence-activated cell sorting

Fluorescence-activated cell sorting (FACS) was performed as described (*32*). Cells were serum-starved for 2 hours, treated as indicated, and stained with Alexa 488–conjugated antibodies against phosphorylated ERK (Invitrogen). Fluorescence profiles were measured on a FACSCalibur (BD Biosciences) with CellQuest Pro software. Distribution profiles were produced with FlowJo software (7.2.2). Data fitting was performed with Microsoft Excel and GraphPad Prism.

Models and modeling

The mathematical models were based on mass action models using ordinary differential equations of an adapted version of the core ERK pathway described in (*24*). Two computational models, Feedback Intact and Feedback Broken, were developed to investigate the NFA characteristics of the ERK pathway. The NFA-like model is the Feedback Intact model. Details are supplied in the Supplementary Materials, section 1.

SUPPLEMENTARY MATERIALS

www.sciencesignaling.org/cgi/content/full/3/153/ra90/DC1
Section 1. Models and modeling.
Section 2. Model parameters.
Section 3. SBML files of the models.
References
Fig. S1. Absolute concentrations of Raf-1, MEK, and ERK in COS1 and NIH 3T3 cells.
Fig. S2. Schematic topologies of the models used.
Fig. S3. Schematic of Raf-1 and the Raf-1 mutants used to probe the NFA hypothesis.
Fig. S4. Expression of Flag-tagged Raf-1 and the Raf6A mutant.
Fig. S5. The effects of U0126 on steady-state ppERK abundance with protein concentrations of COS1 cells.
Fig. S6. The NFA effect also stabilizes non–steady-state dynamic systems.
Fig. S7. Dose-dependent ERK activation by different stimuli.
Fig. S8. B-Raf kinase activity is not feedback-inhibited by ERK.
Tables S1 to S3. Model parameters (Excel).
SBML files of the models (XML).

REFERENCES AND NOTES

1. M. Raman, W. Chen, M. H. Cobb, Differential regulation and properties of MAPKs. *Oncogene* **26**, 3100–3112 (2007).
2. R. Heinrich, B. G. Neel, T. A. Rapoport, Mathematical models of protein kinase signal transduction. *Mol. Cell* **9**, 957–970 (2002).
3. H. M. Sauro, B. N. Kholodenko, Quantitative analysis of signaling networks. *Prog. Biophys. Mol. Biol.* **86**, 5–43 (2004).
4. M. A. Savageau, *Biochemical Systems Analysis. A Study of Function and Design in Molecular Biology* (Addison-Wesley Pub. Co., Reading, MA, 1976).
5. W. Kolch, Coordinating ERK/MAPK signalling through scaffolds and inhibitors. *Nat. Rev. Mol. Cell Biol.* **6**, 827–837 (2005).
6. P. J. Roberts, C. J. Der, Targeting the Raf-MEK-ERK mitogen-activated protein kinase cascade for the treatment of cancer. *Oncogene* **26**, 3291–3310 (2007).
7. A. S. Dhillon, A. von Kriegsheim, J. Grindlay, W. Kolch, Phosphatase and feedback regulation of Raf-1 signaling. *Cell Cycle* **6**, 3–7 (2007).
8. C. Wellbrock, M. Karasarides, R. Marais, The RAF proteins take centre stage. *Nat. Rev. Mol. Cell Biol.* **5**, 875–885 (2004).
9. H. S. Black, Stabilized feedback amplifiers. *Bell Syst. Tech. J.* **13**, 1–18 (1934).
10. G. Palumbo, S. Pennisi, *Feedback Amplifiers: Theory and Design* (Kluwer Academic, Boston/Dordrecht/London, 2002).
11. E. Douville, J. Downward, EGF induced SOS phosphorylation in PC12 cells involves P90 RSK-2. *Oncogene* **15**, 373–383 (1997).
12. M. K. Dougherty, J. Muller, D. A. Ritt, M. Zhou, X. Z. Zhou, T. D. Copeland, T. P. Conrads, T. D. Veenstra, K. P. Lu, D. K. Morrison, Regulation of Raf-1 by direct feedback phosphorylation. *Mol. Cell* **17**, 215–224 (2005).
13. M. L. Samuels, M. J. Weber, J. M. Bishop, M. McMahon, Conditional transformation of cells and rapid activation of the mitogen-activated protein kinase cascade by an estradiol-dependent human raf-1 protein kinase. *Mol. Cell. Biol.* **13**, 6241–6252 (1993).
14. S. P. Davies, H. Reddy, M. Caivano, P. Cohen, Specificity and mechanism of action of some commonly used protein kinase inhibitors. *Biochem. J.* **351**, 95–105 (2000).
15. M. F. Favata, K. Y. Horiuchi, E. J. Manos, A. J. Daulerio, D. A. Stradley, W. S. Feeser, D. E. Van Dyk, W. J. Pitts, R. A. Earl, F. Hobbs, R. A. Copeland, R. L. Magolda, P. A. Scherle, J. M. Trzaskos, Identification of a novel inhibitor of mitogen-activated protein kinase kinase. *J. Biol. Chem.* **273**, 18623–18632 (1998).
16. W. R. Burack, T. W. Sturgill, The activating dual phosphorylation of MAPK by MEK is nonprocessive. *Biochemistry* **36**, 5929–5933 (1997).
17. M. Schilling, T. Maiwald, S. Hengl, D. Winter, C. Kreutz, W. Kolch, W. D. Lehmann, J. Timmer, U. Klingmuller, Theoretical and experimental analysis links isoform-specific ERK signalling to cell fate decisions. *Mol. Syst. Biol.* **5**, 334 (2009).
18. N. I. Markevich, J. B. Hoek, B. N. Kholodenko, Signaling switches and bistability arising from multisite phosphorylation in protein kinase cascades. *J. Cell Biol.* **164**, 353–359 (2004).
19. J. E. Ferrell Jr., E. M. Machleder, The biochemical basis of an all-or-none cell fate switch in *Xenopus* oocytes. *Science* **280**, 895–898 (1998).
20. J. P. Mackeigan, L. O. Murphy, C. A. Dimitri, J. Blenis, Graded mitogen-activated protein kinase activity precedes switch-like c-Fos induction in mammalian cells. *Mol. Cell. Biol.* **25**, 4676–4682 (2005).
21. A. Whitehurst, M. H. Cobb, M. A. White, Stimulus-coupled spatial restriction of extracellular signal-regulated kinase 1/2 activity contributes to the specificity of signal-response pathways. *Mol. Cell. Biol.* **24**, 10145–10150 (2004).
22. J. Yue, J. E. Ferrell Jr., Mos mediates the mitotic activation of p42 MAPK in *Xenopus* egg extracts. *Curr. Biol.* **14**, 1581–1586 (2004).
23. W. S. VanScyoc, G. A. Holdgate, J. E. Sullivan, W. H. Ward, Enzyme kinetics and binding studies on inhibitors of MEK protein kinase. *Biochemistry* **47**, 5017–5027 (2008).
24. B. Schoeberl, C. Eichler-Jonsson, E. D. Gilles, G. Muller, Computational modeling of the dynamics of the MAP kinase cascade activated by surface and internalized EGF receptors. *Nat. Biotechnol.* **20**, 370–375 (2002).
25. L. K. Rushworth, A. D. Hindley, E. O'Neill, W. Kolch, Regulation and role of Raf-1/B-Raf heterodimerization. *Mol. Cell. Biol.* **26**, 2262–2272 (2006).
26. C. A. Pratilas, A. J. Hanrahan, E. Halilovic, Y. Persaud, J. Soh, D. Chitale, H. Shigematsu, H. Yamamoto, A. Sawai, M. Janakiraman, B. S. Taylor, W. Pao, S. Toyooka, M. Ladanyi, A. Gazdar, N. Rosen, D. B. Solit, Genetic predictors of MEK dependence in non-small cell lung cancer. *Cancer Res.* **68**, 9375–9383 (2008).
27. D. B. Solit, L. A. Garraway, C. A. Pratilas, A. Sawai, G. Getz, A. Basso, Q. Ye, J. M. Lobo, Y. She, I. Osman, T. R. Golub, J. Sebolt-Leopold, W. R. Sellers, N. Rosen, BRAF mutation predicts sensitivity to MEK inhibition. *Nature* **439**, 358–362 (2006).
28. N. Dumaz, R. Hayward, J. Martin, L. Ogilvie, D. Hedley, J. A. Curtin, B. C. Bastian, C. Springer, R. Marais, In melanoma, *RAS* mutations are accompanied by switching signaling from BRAF to CRAF and disrupted cyclic AMP signaling. *Cancer Res.* **66**, 9483–9491 (2006).
29. A. A. Adjei, E. K. Rowinsky, Novel anticancer agents in clinical development. *Cancer Biol. Ther.* **2**, S5–S15 (2003).
30. J. S. Sebolt-Leopold, J. M. English, Mechanisms of drug inhibition of signalling molecules. *Nature* **441**, 457–462 (2006).
31. J. Lovric, S. Dammeier, A. Kieser, H. Mischak, W. Kolch, Activated raf induces the hyperphosphorylation of stathmin and the reorganization of the microtubule network. *J. Biol. Chem.* **273**, 22848–22855 (1998).
32. S. D. Santos, P. J. Verveer, P. I. Bastiaens, Growth factor-induced MAPK network topology shapes Erk response determining PC-12 cell fate. *Nat. Cell Biol.* **9**, 324–330 (2007).

33. **Acknowledgments:** We thank T. Gilbey for help with the FACS analysis and J. Kamburapola for help with the LI-COR gels. **Funding:** This work was supported by a DTI Beacons Project, Cancer Research UK, Engineering and Physical Sciences Research Council Basic Technology research grant EP/E032745/1, Science Foundation Ireland grant no. 06/CE/B1129, and FP7 Marie Curie fellowship no. 236758 to M.B. **Author contributions:** O.E.S., J.G., and A.P. performed the experiments; R.O., V.V., and M.B. did the mathematical modeling; W.K., B.K., M.C., and D.G. designed the study; and W.K., R.O., and M.B. wrote the manuscript. **Competing interests:** The authors declare that they have no competing interests.

Submitted 24 May 2010
Accepted 3 December 2010
Final Publication 21 December 2010
10.1126/scisignal.2001212
Citation: O. E. Sturm, R. Orton, J. Grindlay, M. Birtwistle, V. Vyshemirsky, D. Gilbert, M. Calder, A. Pitt, B. Kholodenko, W. Kolch, The mammalian MAPK/ERK pathway exhibits properties of a negative feedback amplifier. *Sci. Signal.* **3**, ra90 (2010).

Abstracts

One-sentence summary: Analysis of ERK pathway circuitry suggests appropriate targets for inhibition, providing a guide for drug development.

Editor's Summary:
Biological Circuits Inform Drug Development

The mitogen-activated protein kinase (MAPK) pathway involves a three-tiered kinase module, which amplifies the signal. Many cells also have negative feedback loops from the last kinase in the module to various points upstream in the pathway. Sturm *et al*. showed that, with negative feedback loops, the MAPK module results in a system like that of a negative feedback amplifier (NFA), which is an engineering design that smoothens the output to changes in input and makes a system robust to change. These NFA-like properties may explain why some cells are sensitive to inhibition of the second kinase in the cascade (they lack feedback loops), whereas other cells are resistant to inhibition at this point (their feedback loops are intact). These results also have implications for drug development, because inhibitors that target components that are outside the NFA are more effective at inhibiting the pathway.